HiSST: 2nd International Conference on
High-Speed Vehicle Science & Technology

11–15 September 2022, Bruges, Belgium

# On the use of random inflow disturbances to simulate transitional hypersonic wind tunnel experiments.

*Mathieu Lugrin* [1]

## Abstract

A direct numerical simulation of the transitional flow around an axisymetrical compression ramp at Mach 5 is conducted for flow conditions corresponding to an experiment of Lugrin et al., 2022. The flow is excited using a random forcing approach (white noise on density), with a noise magnitude chosen to match the time averaged separation size data from the experiments. Unsteady numerical and experimental results are then compared to assess the ability of the random forcing approach to simulate the receptivity process in conventional wind tunnel experiments for such complex flow where multiple mechanisms are present. The computation reproduces the experimental mean flow and turbulent spectrum very precisely. However, the injected noise is found to be biased towards high-frequency and not representative of the R2Ch free-stream fluctuations, which leads to strong discrepancies in the pressure fluctuations spectrum in the laminar part of the flow. As such, the random forcing approach may introduce a bias towards some non-linear breakdown mechanisms that may be different from the one at play in the experiments.

Keywords: *manuscript, latex, template, example*

## Nomenclature

*Latin*

$Re_L$ – Reynolds Number based on cylinder length
$P$ – Pressure
$T$ – Temperature
$A$ – Amplitude of the noise
$r_n$ – Gaussian filtered normalised random number
LST – Linear Stability Theory
DNS – Direct Numerical Simulation

*Greek*

$\rho$ – Density
$\Delta t$ – Time step
$\Delta.+$ – Spacing of the grid in wall unit

*Superscripts*

$'$ – Fluctuations

*Subscripts*

$\infty$ – Freestream quantity
$st$ – Stagnation quantity

## 1. Introduction

Predicting hypersonic laminar turbulent transition remains one of the main challenges for the proper design of hypersonic vehicles. Due to the strong variation of thermal and mechanical loads caused by transition, small uncertainty on the transition location leads to a severe increase in the design margins. Since the study of Morkovin et al. (1994), it is known that the most probable road to transition in hypersonic flow is through linear amplification of convective instabilities (primary mode growth). For that reason, linear instabilities at the origin of transition have been extensively studied in the past using methods such as Linear Stability Theory (LST), one good example being the work of Mack (1975). Then, both to validate the LST results and to get insight on the non-linear interactions that are involved in the latter stage of the transition processes, Direct Numerical Simulations (DNS) were conducted. Traditionally, those are ”controlled” simulations, where one or more particular modes of interest, or their optimal forcings (*i.e.* the optimal perturbation to excite a particular linear mechanism at a given frequency), are injected with a given amplitude (see for instance the work of Franko and Lele (2014) and Franko and Lele (2013)). Then the evolution of the energetic content of the modes, and of their

[1]*DAAA, ONERA, Paris Saclay University, F-92190 Meudon - France, mathieu.lugrin@onera.fr*

secondary instabilities, is studied. While this allows for a fine monitoring of the modes and thus a profound understanding of the energy transfer and amplification mechanisms, those simulations are not representative of either flight, nor wind-tunnel experiments, as the receptivity process is completely bypassed by injecting the instabilities directly in the simulation.

Today, the reproduction of the receptivity process remains one of the main problem facing researchers trying to accurately simulate flight, or wind tunnel, experiments. In opposition to "controlled" DNS, where the injected modes are always present with a given amplitude, the data acquired during transitional experiments shows that the state of boundary layer is very intermittent (see for instance the experimental results shown by Hader and Fasel (2018), or the flight results from Juliano et al. (2015) on the HIFiRE 5 geometry), hinting that the receptivity is constantly changing in time, and thus that the forcing is a statistically complex function in time. The free-stream perturbations present in flight are unknown, there are several hypotheses either linked with atmospheric turbulence, or the presence of aerosols in the flow, but the question is still completely open. There is more data available for wind tunnel noise than flight. For instance, the review of Schneider (2008) on the development of the BAM6QT quiet tunnel provides a good overview of the complexity of the tunnel noise in conventional wind tunnels, with perturbations coming from upstream elements, as well as noise radiated by turbulent boundary layers. In addition to the temporal complexity of the free-stream perturbations, this give insight on its complicated spatial spectrum, with entropic, vortical and acoustic disturbances (Kovasznay, 1953) of different length and shape. Recently, in the scope of the NATO-AVT 240 working group, coordinated experimental and numerical effort were conducted to study the free-stream disturbances in conventional wind tunnels (Duan et al., 2019). Those efforts led to the conclusion that the free-stream noise is dominated by acoustic fluctuations emitted by the turbulent nozzle boundary layer, which are themselves dominated by wave propagating at a certain angle. However, other results, such as the experimental qualification of the VKI H3 wind tunnel by Masutti et al. (2011) tend to show that other type of disturbances (*e.g.* entropic spots), even if less energetic, are also present in the free-stream flow of conventional wind tunnels.

In this context, the numerical reproduction of transitional wind tunnel experiments faces the problematic of the proper definition of the inlet conditions, which should be representative of the free-stream fluctuations of the wind tunnel, without having access to enough information on those perturbations (ideally one would need a complete temporal and spatial spectrum, for the whole state vector). And while some recent approach using input data from a direct numerical simulation of a wind tunnel nozzle boundary layer (and thus the radiated acoustic noise) from Goparaju et al. (2022) showed promising results, they are still very preliminary, and do not cover the whole perturbation range (acoustic only, without the low-frequency contribution of some other elements).

To address the receptivity problem, more and more researchers are using random inflow disturbances to try to recreate the wind tunnel environment. Those inflow disturbances can take several forms, such as wall momentum forcings (Chen et al., 2022; Knutson et al., 2021; Zhu et al., 2022), acoustic waves (Cerminara et al., 2018) , pressure disturbances (Goparaju and Gaitonde, 2021; Hader and Fasel, 2018), or as density perturbations (Leinemann et al., 2021; Lugrin et al., 2021). One common feature, however, is that the spectral content of the noise is chosen broadband, at least in the temporal domain. Those broadband forcing are often presented as a way to let the flow select and amplify the dominant instabilities without choosing a dominant mechanism *a priori*. They also have the advantage of properly reproducing the intermittent characteristic of real life free-stream fluctuations. Hader and Fasel (2018) presented very promising results on the numerical reproduction of a BAM6QT experiment on a flared cone using broadband pressure disturbances, and argued that the random inflow disturbance is a good approach to model the free-stream noise of wind tunnels for which there is not enough data available. The free-stream problem would then be reduced to only one parameter, the amplitude of the noise, which can be easily optimized to match experimental results. However, given the simplified form of such noise, one could wonder whether it can be used to accurately reproduce more complex experiments, where multiple mechanisms are present and competing in the flow, given the fact that each of those mechanisms may have a different receptivity to the injected noise.

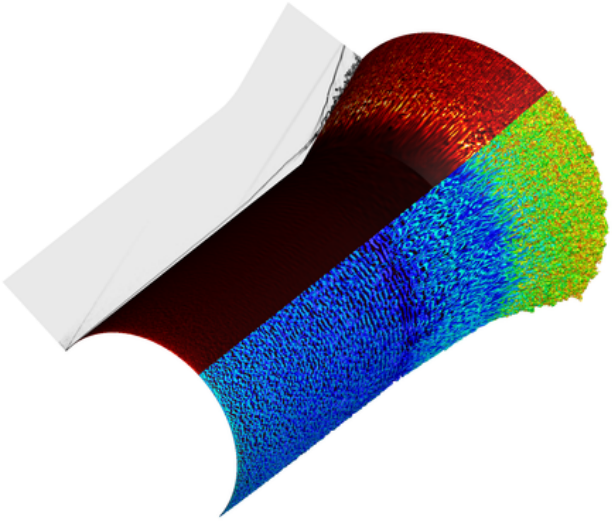

Fig 1. Qualitative illustration of the DNS: isosurface of Q criterion coloured by density, heat-fluxes map at the wall and numerical Schlieren visualisation (from an instantaneous snapshot).

The goal of the article is to assess whether the random inflow disturbances approach is a viable solution to study the transition process happening in wind tunnel experiments of complex multimode hypersonic flows. To accomplish that, a direct numerical simulation with random inflow disturbances of one of the experimental run of Lugrin et al. (2022) is conducted. This case is chosen for multiple reasons: first, at least 3 different primary linear instabilities may be involved in the transition process, first, second and mixing layer modes (Lugrin et al., 2021). For this reason, this case strongly differs from the one presented by Hader and Fasel (2018), which was second mode dominated. This is actually critical, as for the mono-mechanism case, as long as the injected perturbation is not overwhelmingly biased towards another mechanism, one can expect that for a certain amplitude, the injected noise will excite the instability in the same way as the free-stream perturbation of the wind tunnel. For multi-mechanism cases, this is not the case anymore, as a given amplitude may give the correct excitation of one of the mechanisms, but not the other due to the different projection of the injected noise on the optimal forcing of the different instabilities. The second reason to choose this case, is the fact that the mean-flow is strongly impacted by the transition process. Lugrin et al. (2021) have shown that the size of the bubble is strongly correlated with the transition onset, and thus with the level of injected perturbation. This means that the amplitude of the random forcing can simply be chosen as the one that leads to the correct recirculation region size in the simulation. This metric has the advantage to be very well quantified in the experiments.
It is important to note here that the objective of this article is not to study the transition process, nor discuss the physical mechanisms at play in the flow, as this work has already been done by Lugrin et al. (2021) for a similar configuration. The objective here focus on the possibility to accurately reproduce wind tunnel experiment of somewhat complex flow numerically by using a random inflow disturbance. Compared to this previous study, to better reproduce the experimental setup, a new direct numerical simulation is conducted, using a larger domain span, a different noise amplitude and a less dissipative numerical scheme that will be described later.

## 2. Numerical setup and method

The chosen configuration is a reproduction of the $Re_L = 1.1 \times 10^6$ run from Lugrin et al. (2021) (run 1). The free-stream Mach number is $M_\infty = 5$ and the stagnation temperature and pressure are the one from the wind tunnel run : $T_{st} = 547$ K, $P_{st} = 4.14 \times 10^5$ Pa respectively. The geometry is a hollow-cylinder of diameter $D = 131$ mm and length $L = 252$ mm, followed by a $15$-degree flare. The total length of

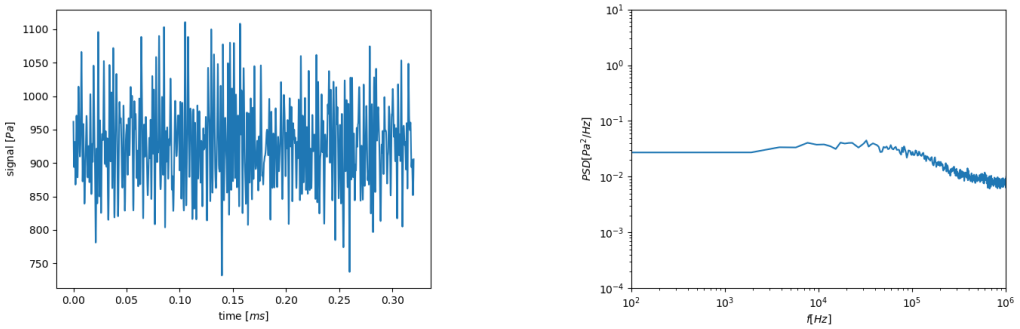


(a) (b)

Fig 2. Temporal (a) and spectral (b) content of the wall pressure fluctuations caused by the noise just after the injection plane.

the model is $350$ mm. A structured mesh $1600 \times 220 \times 1800$ spanning over an angular section of $180°$ of the cylinder-flare configuration with periodic boundary conditions is used. This large domain ensures that the selection of the dominant instabilities is not impacted by the selective filtering of the azimuthal wavenumber imposed by the periodicity. To simplify the computation, the leading edge is supposed to be perfectly sharp and is thus not meshed. Standard supersonic inflow, farfield and outflow conditions are used and the temperature of the no-slip wall is fixed to $290$ K to better reproduce the experimental setup. The grid spacings correspond to the DNS best practice, even in the turbulent region ($\Delta_r^+$ at wall$< 0.5$, $\Delta_x^+ < 8$, $r\Delta_\theta^+ < 5$). An isosurface of the Q criterion coupled to a wall heat-fluxes map and numerical Schlieren visualisation of one snapshot from the DNS is presented in figure 1.

The DNS of the 3D unsteady flow is performed using ONERA's high-performance finite volumes multi-block structured FAST (Flexible Aerodynamic Solver Technology) which solves the compressible Navier–Stokes equations (Péron et al., 2017). The time integration is conducted using an explicit third order, three steps low storage Runge-Kutta integration with a timestep of $\Delta t = 8 \times 10^{-9}$s, ensuring a CFL number of less than 0.5 in the whole domain. The viscous fluxes are computed using a second order accurate centered scheme. For the convective fluxes, to further ensure that the instabilities are correctly resolved, a low dissipation version of the AUSM+P scheme based on the work of Mary and Sagaut (2002) and Garnier (2009) is used. The scheme is based on two sensors, one to detect numerical oscillations (see Mary and Sagaut (2002)) and another one to detect discontinuities in the flow (see Hendrickson et al. (2018)). When strong discontinuities are detected, the scheme is similar to a Roe scheme (Roe, 1981) with an approximation of the dissipation term using the spectral radius of the Roe matrix. Otherwise, if numerical oscillations are detected, the scheme behaves similarly to a standard AUSM+P scheme, with a dissipation proportional to the velocity of the fluid. Finally, when no discontinuities nor numerical oscillations are detected, the scheme is a purely centered second order accurate scheme. This approach, which is similar to the one proposed by Reynaud et al. (2021) ensures that dissipation is only used where it is needed to stabilize the computation. This leads to a better discretization of the high-frequency content of the simulation, including injected noise, transitional instabilities and turbulent structures.

The random disturbance approach used here is similar to the one presented by Lugrin et al. (2022). White noise is injected in the density field in a plane ($j \in [0, 60]$ for the wall normal direction and $k \in [0, 1800]$ azimuthal direction) 4 cells downstream of the inlet boundary condition :

$$\rho'[j,k] = \rho[j,k](1 + Ar_n[j,k]), \tag{1}$$

with $\rho$ the density, $r_n$ a random number which has been Gaussian filtered (kernel spanning over 8 cells) to suppress the very-low wavelength oscillation. The amplitude $A$ being the only free parameter of the noise. The noise is updated every 15 iterations.

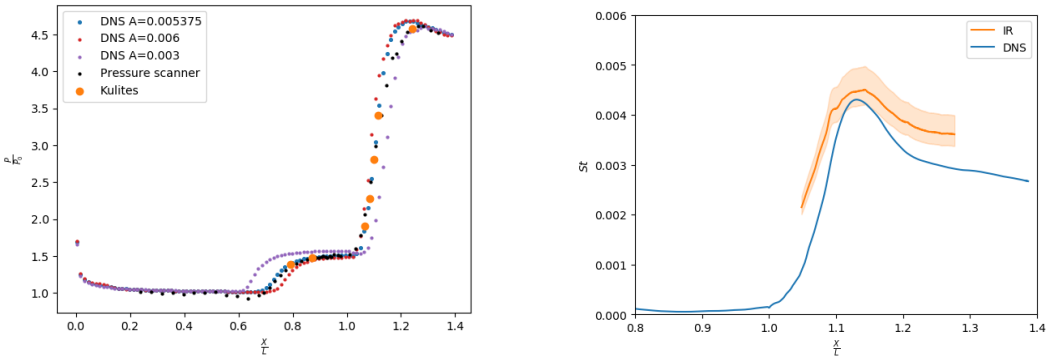


(a) (b)

Fig 3. Comparison of (a) the wall pressure distribution along the geometry, the uncertainty in the pressure scanner (black-dot) measurements is $\pm 10\%$ (error bars not shown), (b) the wall Stanton number from the simulation and the experiments.

One can note here that this noise is different from the one presented by Hader and Fasel (2018) as it is not a pressure perturbation. Two points can be clarified about that: first, the spectral content of the noise is still very similar, as it is broadband (*i.e.* as white as the numerical scheme can resolve). Then, the injection of the noise on the density term brings a bit more generality to the perturbation (Leinemann et al., 2021), as it creates not only acoustic, but also vortical and entropic fluctuations. Figure 2 presents the the pressure fluctuations caused by the noise just after the injection plane, showing the broadband characteristic of the noise.

## 3. Results

### 3.1. Determination of the adequate level of free-stream disturbances

Now that the form of the injected noise is fixed, one needs to decide on the amplitude of perturbations to use to reproduce the experiments.

As stated in the introduction, the error on the recirculation region size is chosen as the objective function to minimize for the optimization of the noise level. This choice is motivated by two reasons: first, Lugrin et al. (2021) showed that it is very sensitive to the level of perturbation injected in the flow for an almost similar case (slightly higher Reynolds number). Second, it is very well described in the experiments because of the high number of pressure taps (50) and Kulite sensors (7) that were used. Thus, the level of noise is chosen such that it leads to a correct reproduction of the separated region size. A simple optimization of the noise amplitude is conducted by computing mean-flow of the DNS for different level of noise. This optimization led to an optimal amplitude of $A = 0.005375$.

Figure 3 presents the time-averaged results from the simulation and the experiments. Figure 3 (a) presents the time averaged pressure distribution for a line of static pressure probes at different longitudinal positions along the geometry, it shows that the chosen level of noise lead to very precise reproduction of the bubble size, with correct position of the separation (first increase in pressure from $\frac{P}{P_\infty} = 1$ to roughly $1.5$) and reattachment point (second increase in pressure after the plateau at $1.5$), two other amplitudes of injected noise are also displayed to illustrate the strong impact of the disturbances on the mean flow. Given the previous results of Lugrin et al. (2021), which showed that the transition for that kind of flow was happening in a very abrupt manner at the reattachment point, the correct match of the bubble topology means that the transition onset is correctly predicted by the simulation. Figure 3 (b) presents the temporal and azimuthal averages of the Stanton numbers in the reattachment region, it shows that the peak heat-flux position and value are correctly captured by the DNS. The Stanton number, however, seems to be slightly underestimated in the turbulent region. This discrepancy may be linked with the wall temperature being approximated at $290$ K in the simulation. Overall, those figures prove that the injected disturbances allow for an accurate prediction of the time-averaged values

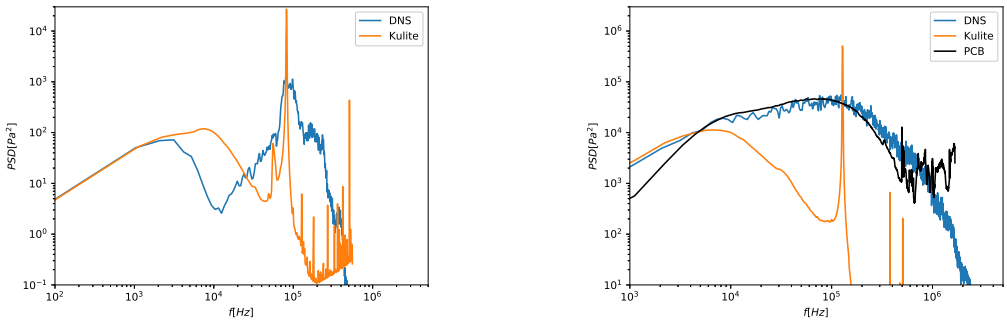


(a) (b)

Fig 4. Comparison of the numerical and experimental pressure power spectral densities inside the separated region ($\frac{X}{L} = 0.87$) (a) and after the reattachment ($\frac{X}{L} = 1.1$) (b). Note the resonance of the Kulite sensor just before $100$ kHz.

available in the experiments.

### 3.2. Transitional instabilities

Once the level of noise is chosen and the experimental mean-flow measurements are correctly reproduced by the simulation, one can confront the unsteady pressure data from the experiments to the one from the DNS. Given the previously discussed accuracy on the mean-flow reproduction, one can expect that the exact same linear mechanisms will be at play in the DNS and the experiment, and thus, any discrepancies in the unsteady pressure data can be attributed to differences in the receptivity process. Note that in addition to unsteady pressure measurements, Lugrin et al. (2022) provided infrared imaging results on the streaky pattern appearing in the reattachment region. Given that there are uncertainties on the mechanisms a play in the amplification of those streaks, and that there may be other receptivity mechanisms involved which are not reproduced in this simulation (namely receptivity to the leading edge geometrical imperfections, that may lead to the appearance of Görtler vortices), those results will not be used to assess the validity of the random disturbances approach.

Figure 4 (a) presents a comparison of pressure power spectral densities for a sensor located inside the recirculation region upstream of the transition point. First, the spectrum match for the very low frequency content. For frequencies higher than $2$ kHz, the DNS spectrum starts to depart from the experimental one, as it displays lower levels of energy. Then for frequencies higher than roughly $30$ kHz the DNS energetic content increases and becomes greater than the experimental value. One has to be careful when interpreting the results around $80 - 100$ kHz as the huge peak in the experimental spectrum is due to the resonance of the sensor membrane. The main information that we can get from figure 4 (a) is that the DNS seems to contain more energetic structures are higher frequencies, while the experiments display higher level of energy for low frequencies. The most amplified instabilities in the DNS and experiments are not matching, nor the general shape of the spectrum.

Figure 4 (b) presents the same results for sensors located on the flare, in a turbulent region of the flow, note that for this location, two sensors are available, including a PCB sensor which allows to interpret the results from $10$ kHz up to $300$ kHz. Note that for high-frequency content (higher than $20 - 30$ kHz), the PCB sensor is more accurate than the Kulite sensor. This figure shows that downstream of the transition location, the DNS results are exactly similar to the experimental on the whole frequency range that can be experimentally measured. While this does not bring information on whether the transition process is the same in the simulation and the experiments, it is still an important result as it shows that even if the instabilities upstream of the transition point are not matching, the fully turbulent spectrum downstream of the transition point can be accurately reproduced numerically. The results of figure 4 (b) should also be kept in mind while interpreting the results shown in figure 4 (a) as the signal from the Kulite sensor decreases for frequencies higher than $10$ kHz.

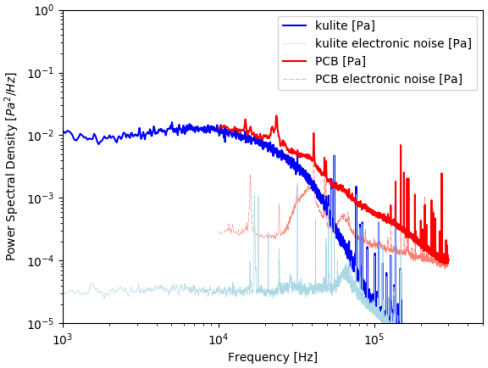


Fig 5. Spectral content of the free-stream noise, measured by a Kulite and PCB sensors mounted on a 5 degree half angle sharp cone.

Keeping that limitation in mind and going back to the results of figure 4 (a) one can conclude that the white noise injected in the simulation is lacking low frequency content and may be biased towards high-frequency. This can be further discussed when considering the free-stream pressure fluctuations spectrum presented in figure 5. This spectrum was measured for similar flow conditions using a $5°$ half angle sharp cone equipped with a Kulite and a PCB flush mounted as close as possible to the tip. While this setup is not optimal, as the free-stream fluctuations still have to pass through a weak attached shock and a boundary layer (which transfer function is unknown) before being measured, it can still bring interesting information on the spectral content (in time only) of the free-stream noise of R2Ch. This spectrum, compared to the numerical noise spectrum presented in figure 2 (b) confirms the assumption that the numerical white noise is indeed biased toward high-frequency. For frequencies higher than $10$ kHz the energetic content of the R2Ch free-stream noise starts to decrease, while the energetic content of the noise stays constant. This bias may explain why there is an overestimation of the energetic content of the instabilities in the $30 - 150$ kHz range in the DNS, as the free-stream noise energetic content is one to two orders of magnitude smaller in that range than in the $1 - 10$ kHz range. However, it does not explain why the DNS underestimates the energetic content around $10$ kHz, as the free-stream fluctuations spectrum displays no increase in energetic content in that range and seems very similar to the white noise spectrum. One can make three hypotheses, on the potential origin of this mismatch. First, it could be linked with the complexity of the spatial spectrum of the noise. Depending on its spatial shape, the noise may or may not project on the optimal forgings of the linear instabilities, and thus, the temporal spectrum by itself does not bring enough information to conclude on the receptivity of the different instabilities. It is not impossible that the instability developing in that frequency range are strongly excited by some fluctuations present in the R2Ch free-stream noise, just because the spatial shape of the noise strongly resemble the optimal forcing of such instabilities. Secondly, it is possible that the instability in this range are excited by free-stream disturbances that are not measured by the pressure sensor mounted on the cone (*e.g.* entropic or vortical structures). Given the relative low frequency of those instabilities, they may be excited by disturbances that are not radiated by the turbulent boundary layer on the nozzle wall, but emitted by parts (valve, settling chamber, *etc*) upstream of the nozzle (Schneider, 2008). To confirm this assumption, one would need more precise measurements of all the different perturbations present in the flow, using for instance a double hot-wire (Masutti et al., 2011). If it is confirmed, it would mean that even with advanced noise models, following for example the work of Goparaju et al. (2022) which used a reduced order model of the noise radiated by the turbulent boundary layer, one could still miss important instabilities and transitional mechanisms in the numerical reproduction of experiments. Last, different non-linear interaction between the modes may be at play in the flow. If there is a difference in receptivity in the experiment and the simulation, the linear modes may reach their saturation at different location and thus the non-linear redistribution of the energy may be strongly impacted by a difference in the injected noise.

From these results, and even if the transition onset and the turbulent spectrum are correctly predicted, one can wonder if the transition is actually happening in the same way in the DNS and the experiments, given that the dominant mechanisms in the laminar region of the flow are at different frequencies, meaning that different linear instabilities could reach the non-linear stage in both cases at different locations. For that reason, it is very unclear if the transition scenario presented by Lugrin et al. (2021) is still relevant in the experiments.

## 4. Conclusion

To conclude, a DNS of the transitional flow around an axisymetrical compression ramp at Mach 5 for flow conditions corresponding to an experiment of Lugrin et al. (2022) has been conducted using a random disturbance injection at the inlet. This case was chosen as it is a good way to benchmark whether the random disturbances approach is a suitable way to reproduce the unknown free-stream disturbances present in hypersonic wind tunnels. Given the fact that the mean flow is very sensitive to the transition onset, the disturbance amplitude is chosen such that the simulation accurately predict the mean flow from the experiments. With the correct perturbation amplitude, the DNS is found to reproduce the experimental mean flow very precisely. The DNS also provides the correct pressure spectrum in the turbulent region of the flow. However, the fluctuation spectra in the laminar part of the flow differs between the DNS and the experiment. These discrepancies bring doubt on the ability of the DNS to capture the proper experimental transition scenario. The origin of this mismatch can be fully attributed to a difference in the receptivity process and as such, those results display how limited the random disturbance approach is for complex cases (both in terms of free-stream fluctuations, and flow instabilities). While this approach allows to reproduce some important characteristics of the flow, such as broadband mode amplification, or intermittent behavior, it is found to be biased toward high-frequency and not representative of the particularity of tunnel noises, which led to strong discrepancies in the energetic level of the instabilities. Note that while in the present paper, it was chosen to use a density forcing, some other author prefer momentum forcing, acoustic waves or pressure disturbances, the same discussion about both the temporal and spatial content of the noise would hold for other kind of disturbances. Another conclusion that can be drawn is that an optimization of the noise based solely on mean-flow quantities is not a proper solution, as even when the mean-flow is strongly impacted by the transition process, this only impose the correct transition onset and not the mechanisms at play. This is especially important given the recent development towards the use of variational optimization method to reproduce hypersonic transitional experiments (Buchta and Zaki, 2021).

In this context, to accurately reproduce transitional hypersonic experiments, future efforts should go towards using higher fidelity model of wind tunnel free-stream disturbances. First, numerical simulation of full-scale nozzle (Duan et al., 2019) seems to be a good solution to properly quantify and model the acoustic noise radiated from the nozzle boundary layer. However, this may not be enough for blowdown facilities, where free-stream disturbances of other origins may also be present. Because of that, proper experimental characterization of the free-stream disturbances are needed. While some results are very promising as they start to bring data not just on pressure fluctuations, but also on entropic and vortical spots (Masutti et al., 2011), the available data remains very sparse. Experimental efforts should go towards reducing the sparsity of such data, with a particular focus on discriminating noises of different origin and quantifying the spatial characteristics of the fluctuations.

The author which to thank Eric Garnier, Ivan Mary and Cedric Content for the discussions about the dissipation of second order numerical schemes. The DNS was performed thanks to a 1M CPU hours allocation for young researchers from ONERA.

## References

Buchta, D. A. and T. A. Zaki (2021). "Observation-infused simulations of high-speed boundary-layer transition". In: *Journal of Fluid Mechanics* 916 (2021) (cit. on p. 8).

Cerminara, A., A. Durant, T. André, N. Sandham, and N. J. Taylor (2018). "DNS of acoustic receptivity and breakdown in a Mach 6 flow over a generic forebody". In: *2018 AIAA Aerospace Sciences Meeting*. 2018, p. 0348 (cit. on p. 2).

Chen, X., S. Dong, G. Tu, X. Yuan, and J. Chen (2022). "Boundary layer transition and linear modal instabilities of hypersonic flow over a lifting body". In: *Journal of Fluid Mechanics* 938 (2022) (cit. on p. 2).

Duan, L. et al. (2019). "Characterization of freestream disturbances in conventional hypersonic wind tunnels". In: *Journal of Spacecraft and Rockets* 56.2 (2019), pp. 357–368 (cit. on pp. 2, 8).

Franko, K. J. and S. Lele (2014). "Effect of adverse pressure gradient on high speed boundary layer transition". In: *Physics of Fluids* 26.2 (2014), p. 24106 (cit. on p. 1).

Franko, K. J. and S. K. Lele (2013). "Breakdown mechanisms and heat transfer overshoot in hypersonic zero pressure gradient boundary layers". In: *Journal of Fluid Mechanics* 730 (2013), pp. 491–532 (cit. on p. 1).

Garnier, E. (2009). "Stimulated detached eddy simulation of three-dimensional shock/boundary layer interaction". In: *Shock waves* 19.6 (2009), pp. 479–486 (cit. on p. 4).

Goparaju, H. and D. V. Gaitonde (2021). "Transition to turbulence on hypersonic flat plates induced by stochastic forcing". In: *AIAA Scitech 2021 Forum*. 2021, p. 1738 (cit. on p. 2).

Goparaju, H., Y. Liu, L. Duan, and D. V. Gaitonde (2022). "Supersonic transition induced by numerical tunnel disturbances". In: *AIAA SCITECH 2022 Forum*. 2022, p. 1826 (cit. on pp. 2, 7).

Hader, C. and H. F. Fasel (2018). "Towards simulating natural transition in hypersonic boundary layers via random inflow disturbances". In: *Journal of Fluid Mechanics* 847 (2018) (cit. on pp. 2, 3, 5).

Hendrickson, T. A., A. Kartha, and G. V. Candler (2018). "An improved ducros sensor for the simulation of compressible flows with shocks". In: *2018 Fluid Dynamics Conference*. 2018, p. 3710 (cit. on p. 4).

Juliano, T. J., D. Adamczak, and R. L. Kimmel (2015). "HIFiRE-5 flight test results". In: *Journal of Spacecraft and Rockets* 52.3 (2015), pp. 650–663 (cit. on p. 2).

Knutson, A. L., J. S. Thome, and G. V. Candler (2021). "Numerical simulation of instabilities in the boundary-layer transition experiment flowfield". In: *Journal of Spacecraft and Rockets* 58.1 (2021), pp. 90–99 (cit. on p. 2).

Kovasznay, L. S. (1953). "Turbulence in supersonic flow". In: *Journal of the Aeronautical Sciences* 20.10 (1953), pp. 657–674 (cit. on p. 2).

Leinemann, M., C. Hader, and H. F. Fasel (2021). "Direct numerical simulations of the nonlinear boundary layer transition regime on a flat plate at Mach 6". In: *AIAA Scitech 2021 Forum*. 2021, p. 1739 (cit. on pp. 2, 5).

Lugrin, M., S. Beneddine, C. Leclercq, E. Garnier, and R. Bur (2021). "Transition scenario in hypersonic axisymmetrical compression ramp flow". In: *Journal of Fluid Mechanics* 907 (2021), A6. arXiv: 2009.08359 (cit. on pp. 2, 3, 5, 8).

Lugrin, M., F. Nicolas, N. Severac, J.-P. Tobeli, S. Beneddine, E. Garnier, S. Esquieu, and R. Bur (2022). "Transitional shockwave/boundary layer interaction experiments in the R2Ch blowdown wind tunnel". In: *Experiments in Fluids* 63.2 (2022), pp. 1–19 (cit. on pp. 1, 3, 4, 6, 8).

Mack, L. M. (1975). "Linear stability theory and the problem of supersonic boundary- layer transition". In: *AIAA Journal* 13.3 (1975), pp. 278–289 (cit. on p. 1).

Mary, I. and P. Sagaut (2002). "Large Eddy Simulation of Flow Around an Airfoil Near Stall". In: *AIAA Journal* 40.6 (2002), pp. 1139–1145 (cit. on p. 4).

Masutti, D., E. Spinosa, O. Chazot, and M. Carbonaro (2011). "Disturbance level characterization of a hypersonic blow-down facility". In: *41st AIAA Fluid Dynamics Conference and Exhibit* 50.12 (2011), pp. 2720–2730 (cit. on pp. 2, 7, 8).

Morkovin, M. V., E Reshotko, and T Herbert (1994). "Transition in open flow systems – a reassessment". In: *Bull. A. Phys. Soc.* 39 (1994), p. 1882 (cit. on p. 1).

Péron, S., T. Renaud, M. Terracol, C. Benoit, and I. Mary (2017). "An immersed boundary method for preliminary design aerodynamic studies of complex configurations". In: *23rd AIAA Computational Fluid Dynamics Conference, 2017*. 2017, p. 3623 (cit. on p. 4).

 

Reynaud, J., P.-E. Weiss, and S. Deck (2021). "Numerical workflow for scale-resolving computations of space launcher afterbody flows with and without jets". In: *Computers & Fluids* 226 (2021), p. 104994 (cit. on p. 4).

Roe, P. L. (1981). "Approximate Riemann solvers, parameter vectors, and difference schemes". In: *Journal of computational physics* 43.2 (1981), pp. 357–372 (cit. on p. 4).

Schneider, S. P. (2008). "Development of hypersonic quiet tunnels". In: *Journal of Spacecraft and Rockets* 45.4 (2008), pp. 641–664 (cit. on pp. 2, 7).

Zhu, W., D. Gu, W. Si, M. Zhang, S. Chen, C. Smith, Y. Zhu, and C. Lee (2022). "Instability evolution in the hypersonic boundary layer over a wavy wall". In: *Journal of Fluid Mechanics* 943 (2022) (cit. on p. 2).